

**Anomalous  $B$ -meson mixing and baryogenesis**Sean Tulin<sup>1</sup> and Peter Winslow<sup>1,2</sup><sup>1</sup>*Theory Group, TRIUMF, 4004 Wesbrook Mall, Vancouver, British Columbia, V6T 2A3, Canada*<sup>2</sup>*Department of Physics and Astronomy, University of British Columbia, 6224 Agricultural Road, Vancouver, British Columbia, V6T 1Z1, Canada*

(Received 27 May 2011; published 9 August 2011)

There exist experimental hints from the  $B$  sector for  $CP$  violation beyond the standard model (SM) paradigm. An anomalous dimuon asymmetry was reported by the D0 Collaboration, while tension exists between  $B \rightarrow \tau \nu$  and  $S_{\psi K}$ . These measurements, disfavoring the SM at the  $\sim 3\sigma$  level, can be explained by new physics in both  $B_d^0 - \bar{B}_d^0$  and  $B_s^0 - \bar{B}_s^0$  mixing, arising from (1) new bosonic degrees of freedom at or near the electroweak scale, and (2) new, large  $CP$ -violating phases. These two new physics ingredients are precisely what is required for electroweak baryogenesis to work in an extension of the SM. We show that a simple two Higgs doublet model with top-charm flavor violation can explain the  $B$  anomalies and the baryon asymmetry of the Universe. Moreover, the presence of a large relative phase in the top-charm Yukawa coupling, favored by  $B_{d,s}^0 - \bar{B}_{d,s}^0$  mixing, weakens constraints from  $\epsilon_K$  and  $b \rightarrow s\gamma$ , allowing for a light charged Higgs mass of  $\mathcal{O}(100 \text{ GeV})$ .

DOI: 10.1103/PhysRevD.84.034013

PACS numbers: 14.40.Nd, 12.60.Fr

**I. INTRODUCTION**

Precision tests of  $CP$  violation have shown a remarkable consistency with the standard model (SM), where all  $CP$ -violating observables are governed uniquely by the single phase in the Cabibbo-Kobayashi-Maskawa (CKM) matrix [1]. Yet the search continues. Many well-motivated extensions of the SM, such as supersymmetry, contain new sources of  $CP$  violation at the electroweak scale. Furthermore, new  $CP$  violation beyond the CKM phase is likely required to explain the origin of the baryon asymmetry of the Universe.

Recent analyses have suggested that the CKM paradigm may be in trouble. First, the D0 Collaboration has measured the like-sign dimuon asymmetry, arising from  $CP$  violation in the mixing and decays of  $B_{d,s}^0$  mesons, in excess over SM prediction at the  $3.2\sigma$  level [2]. Second, there is tension at the  $\sim 3\sigma$  level between the branching ratio for  $B^+ \rightarrow \tau^+ \nu$  and the  $CP$  asymmetry  $S_{\psi K}$  in  $B_d^0 \rightarrow J/\psi K$  [3,4]. Additionally, CDF and D0 have measured the  $CP$  asymmetry  $S_{\psi \phi}$  in  $B_s^0 \rightarrow J/\psi \phi$ . While their earlier results (each with  $2.8 \text{ fb}^{-1}$  data) showed a  $\sim 2\sigma$  deviation from the SM [5], this discrepancy has been reduced in their updated analyses with more data ( $5.2$  and  $6.1 \text{ fb}^{-1}$ , respectively) [6].

Although further experimental study is required, taken at face value, these anomalies suggest  $CP$  violation from new physics (NP) in the mixing and/or decay amplitudes of  $B_d^0$  and  $B_s^0$  mesons [7]. Recently, the CKMfitter group has performed a global fit to all flavor observables, allowing for arbitrary new physics in  $B_{d,s}^0 - \bar{B}_{d,s}^0$  mixing amplitudes [8]. They conclude that the SM is disfavored at  $3.4\sigma$ , while the data seem to favor NP with large  $CP$ -violating phases relative to the SM in both  $B_d^0$  and  $B_s^0$  mixing. At the level of effective theory, this NP takes the form

$$\mathcal{L}_{\text{NP}} \sim \frac{c_d}{\Lambda^2} (\bar{b}d)^2 + \frac{c_s}{\Lambda^2} (\bar{b}s)^2 + \text{H.c.} \quad (1)$$

These operators can arise from new bosonic degrees of freedom at or near the weak scale, with new large  $CP$ -violating phases [9–12].

It is suggestive that the same NP ingredients, new weak-scale bosons and new  $CP$  violation, can also lead to successful electroweak baryogenesis (EWBG). EWBG, in which the baryon asymmetry is generated during the electroweak phase transition [13–15], is particularly attractive since two out of three Sakharov conditions [16] can be tested experimentally. First, a departure from thermal equilibrium is provided by a strong first-order phase transition, proceeding by bubble nucleation. While this does not occur in the SM [17], additional weak-scale bosonic degrees of freedom can induce the required phase transition; these new bosons can be searched for at colliders. Second, there must exist new  $CP$  violation beyond the SM [18]. This  $CP$  violation must involve particles with large couplings to the Higgs boson, since it is the interactions of those particles with the dynamical Higgs background field that leads to baryon production. Precision tests, such as electric dipole moment searches [19] and flavor observables, can probe directly  $CP$  violation relevant for EWBG. (The third condition, baryon number violation, is provided in the SM by weak sphalerons [20]; however, it is difficult to probe experimentally, since the sphaleron rate is highly suppressed at temperatures below the weak scale.)

If we wish to connect Eq. (1) to EWBG, it is better to generate these operators at one loop, rather than tree level. Constraints on the mass differences  $\Delta M_{d,s}$  in the  $B_{d,s}^0$  systems require that  $\Lambda^2/|c_d| \gtrsim (500 \text{ TeV})^2$  and  $\Lambda^2/|c_s| \gtrsim (100 \text{ TeV})^2$  [21]. For tree-level exchange, it seems unlikely that all three Sakharov conditions can be met at once. Sufficient baryon number generation typically requires

couplings  $\gtrsim \mathcal{O}(10^{-1})$ , such that  $c_{d,s} \gtrsim \mathcal{O}(10^{-2})$ , while a viable phase transition requires  $\Lambda \lesssim 1$  TeV. Therefore, EWBG requires  $\Lambda^2/|c_{d,s}| \lesssim (10 \text{ TeV})^2$ , at odds with  $\Delta M_{d,s}$  constraints. However, if the operators in Eq. (1) arise at one-loop order,  $c_{d,s}$  will have an additional  $1/(4\pi)^2$  loop suppression, allowing for both large couplings and lighter scale  $\Lambda$ , without conflicting with  $\Delta M_{d,s}$  constraints.

In this work, we propose that a simple two Higgs doublet model (2HDM) can account for both anomalous  $CP$  violation in  $B_{d,s}^0$ - $\bar{B}_{d,s}^0$  mixing and EWBG. Previous works have studied  $CP$  violation in  $B_{d,s}^0$ - $\bar{B}_{d,s}^0$  mixing within a 2HDM [9–12]. Our setup, described in Sec. II, is different: we assume the NP Higgs doublet ( $H^+$ ,  $H^0 + iA^0$ ) mediates top-charm flavor violation. In this case, the NP  $B_{d,s}^0$ - $\bar{B}_{d,s}^0$  mixing amplitudes  $(M_{12}^{d,s})_{\text{NP}}$  are generated at one-loop order through charge current interactions mediated by  $H^+$  (similar to Ref. [12]), rather than through tree-level exchange [9–11]. In Sec. III, we compute  $(M_{12}^{d,s})_{\text{NP}}$  in our model. We find the following:

- (i) The best fit values to both  $M_{12}^d$  and  $M_{12}^s$ , from Ref. [8], can be explained in terms of a single NP phase  $\vartheta_{tc}$  (defined below).
- (ii) For large values of  $\vartheta_{tc}$  preferred by  $B_{d,s}^0$ - $\bar{B}_{d,s}^0$  mixing observables, constraints from  $\epsilon_K$  and  $b \rightarrow s\gamma$  are weakened and  $H^\pm$  can be light ( $m_{H^\pm} \sim 100$  GeV).

In Sec. IV, we discuss in detail EWBG in our 2HDM model. We focus on the  $CP$  violation aspects of EWBG, computing the baryon asymmetry in terms of the underlying parameters of our model by solving a system of coupled Boltzmann equations. We find that the parameter region favored by flavor observables (specifically, a large  $\bar{t}_R t_L H^0$  coupling) can easily account for the observed baryon asymmetry. However, the relevant  $CP$ -violating phase is unrelated to the phase  $\vartheta_{tc}$  entering flavor observables. In Sec. V, we summarize our conclusions.

## II. MODEL

In a general (type-III) two Higgs doublet model [22,23], where both Higgs fields couple to each SM fermion, one can perform a field redefinition such that only one Higgs field acquires a real, positive vacuum expectation value (vev) [24]. We denote the two Higgs doublets by

$$H_1 = \begin{pmatrix} G^+ \\ v + \frac{h^0 + iG^0}{\sqrt{2}} \end{pmatrix}, \quad H_2 = \begin{pmatrix} H^+ \\ \frac{H^0 + iA^0}{\sqrt{2}} \end{pmatrix}, \quad (2)$$

where  $h^0$ ,  $H^0$  ( $A^0$ ) are the neutral (pseudo)scalars,  $H^\pm$  is a charged scalar, and  $G^{\pm,0}$  are the Goldstone modes eaten by the electroweak gauge bosons. The vev is  $v \approx 174$  GeV. In general, the physical neutral states can be admixtures of  $h^0$ ,  $H^0$ ,  $A^0$ , depending on the details of the Higgs potential. We neglect mixing in our analysis; in this case,  $H_1$  is exactly an SM Higgs doublet.

The most general Yukawa interaction for  $u$ -type quarks is

$$\mathcal{L}_{\text{yuk}} \supset \bar{u}_R (y_U H_1 + \tilde{y}_U H_2) Q_L + \text{H.c.}, \quad (3)$$

where the left-handed quark doublet is  $Q_L \equiv (u_L, Vd_L)$ . The  $SU(2)_L$  contraction is  $H_i Q_L \equiv H_i^+ (Vd_L) - H_i^0 u_L$ . The  $3 \times 3$  Yukawa matrices  $y_U$  and  $\tilde{y}_U$  couple right-handed  $u$ -type quarks  $u_R \equiv (u, c, t)_R$  to left-handed quarks  $u_L \equiv (u, c, t)_L$  and  $d_L \equiv (d, s, b)_L$ . Working in the mass eigenstate basis, the matrix

$$y_U = \text{diag}(y_u, y_c, y_t) = \text{diag}(m_u, m_c, m_t)/v \quad (4)$$

is a diagonal matrix of SM Yukawa couplings, and  $V$  is the CKM matrix. Analogous Yukawa couplings arise for down quarks and charged leptons:

$$\begin{aligned} \mathcal{L}_{\text{yuk}} \supset & -\bar{d}_R (y_D H_1^\dagger + \tilde{y}_D H_2^\dagger) Q_L \\ & -\bar{e}_R (y_L H_1^\dagger + \tilde{y}_L H_2^\dagger) L_L + \text{H.c.}, \end{aligned} \quad (5)$$

where  $y_D = \text{diag}(y_d, y_s, y_b)$  and  $y_L = \text{diag}(y_e, y_\mu, y_\tau)$  are the SM Yukawa couplings.

The NP Yukawa matrices  $\tilde{y}_{U,D,L}$  can be arbitrary. However, the absence of anomalously large flavor-violating processes provides strong motivation for an organizing principle. In this work, we assume that flavor violation arises predominantly in the top sector. Specifically, we take

$$\tilde{y}_U = \begin{pmatrix} 0 & 0 & 0 \\ 0 & 0 & 0 \\ 0 & \tilde{y}_{tc} & \tilde{y}_{tt} \end{pmatrix}, \quad \tilde{y}_{D,L} = 0. \quad (6)$$

That is, we consider a hierarchical structure, in the spirit of Ref. [23], where the  $t_R t_L$  and  $t_R c_L$  couplings are dominant (with  $|\tilde{y}_{tt}| \gg |\tilde{y}_{tc}|$ ), while others are suppressed. The zeros in Eq. (6) are meant to indicate these subleading couplings that for simplicity we neglect in our analysis. In our setup, flavor violation in meson observables arises at one-loop order through  $H^\pm$  charge current interactions, discussed in the next section.

## III. FLAVOR CONSTRAINTS

Mixing and  $CP$  violation in the  $B_q^0$ - $\bar{B}_q^0$  system ( $q = d, s$ ) is governed by the off-diagonal matrix element  $M_{12}^q - \frac{i}{2} \Gamma_{12}^q$  in the Hamiltonian [25,26], with  $M_{12}^q$  ( $\Gamma_{12}^q$ ) associated with the (anti-)Hermitian part. Only the relative phase  $\phi_q \equiv \arg(-M_{12}^q/\Gamma_{12}^q)$  is physical. The relevant observables are the mass and width differences between the two eigenstates

$$\Delta M_q = 2|M_{12}^q|, \quad \Delta \Gamma_q = 2|\Gamma_{12}^q| \cos \phi_q, \quad (7)$$

and the wrong sign semileptonic asymmetry

$$a_{\text{sl}}^q \equiv \frac{\Gamma(\bar{B}_q^0 \rightarrow \mu^+ X) - \Gamma(B_q^0 \rightarrow \mu^- X)}{\Gamma(\bar{B}_q^0 \rightarrow \mu^+ X) + \Gamma(B_q^0 \rightarrow \mu^- X)} = \frac{|\Gamma_{12}^q|}{|M_{12}^q|} \sin \phi_q. \quad (8)$$

The dimuon asymmetry measured by D0 arises from wrong sign semileptonic decays of both  $B_d^0$  and  $B_s^0$  mesons and is given by  $A_{\text{sl}}^b \approx 0.5a_{\text{sl}}^d + 0.5a_{\text{sl}}^s$  [2].

In the SM, the mixing amplitude  $M_{12}^q$  arises from box graphs, while the  $\Gamma_{12}^q$  comes from tree-level decays. Therefore, it is plausible that NP effects enter predominantly through mixing. Deviations in  $M_{12}^q$  from the SM can be parametrized by

$$M_{12}^q = (M_{12}^q)_{\text{SM}} + (M_{12}^q)_{\text{NP}} \equiv (M_{12}^q)_{\text{SM}} \Delta_q. \quad (9)$$

The consistency of  $\Delta M_{d,s}$  with SM predictions constrains  $|\Delta_{d,s}| \approx 1$ , at the  $\mathcal{O}(20\%)$  level [8], while the dimuon asymmetry measurement disagrees with SM prediction at  $3.2\sigma$  and requires  $\mathcal{O}(1)$  NP phases  $\phi_q^\Delta \equiv \arg(\Delta_q)$  [2]. Phases  $\phi_q^\Delta$  also enter into  $CP$  asymmetries due to interference between  $B_{d,s}^0$  decay amplitudes with and without mixing: e.g., the asymmetry for  $B_d^0 \rightarrow J/\psi K_S^0$  is  $S_{\phi_{K_S}} = \sin(2\beta + \phi_d^\Delta)$ , with CKM angle  $\beta \equiv \arg(-V_{cd}V_{cb}^*V_{td}V_{tb}^*)$ . As emphasized in Ref. [4], the presence of nonzero  $\phi_d^\Delta$  can alleviate tension between  $S_{\phi_{K_S}}$  and  $\text{Br}(B^+ \rightarrow \tau^+\nu)$ , which is sensitive to  $\beta$  but not  $\phi_d^\Delta$ .

To quantify these tensions, the CKMfitter group performed a global fit allowing for arbitrary  $\Delta_{d,s}$  (dubbed ‘‘Scenario I’’), finding that the SM point ( $\Delta_d = \Delta_s = 1$ ) is disfavored at  $3.4\sigma$  [8]. Moreover, their best fit point favors NP  $CP$ -violating phases in both  $B_d^0$  and  $B_s^0$  mixing:  $\phi_d^\Delta = (-12_{-3.4}^{+3.3})^\circ$  and  $\phi_s^\Delta = (-129_{-12}^{+12})^\circ \cup (-51.6_{-9.4}^{+14.1})^\circ$ .<sup>1</sup>

In our model, NP effects enter  $B_{d,s}^0$  observables predominantly through mixing, via box diagrams shown in Fig. 1. We find<sup>2</sup>

$$\Delta_q = 1 + c_{bq} F_1(x_H, x_t)/S_0(x_t) + c_{bq}^2 F_2(x_H, x_t)/S_0(x_t), \quad (10)$$

where

$$c_{ij} \equiv \frac{(\tilde{y}_U V)_{ii} (\tilde{y}_U V)_{ij}^*}{4\sqrt{2} G_F m_W^2 V_{ii} V_{ij}^*}. \quad (11)$$

The  $\bar{t}_R d_L^i H^+$  charge current couplings are  $(\tilde{y}_U V)_{ii} = \tilde{y}_{it} V_{ii} + \tilde{y}_{ic} V_{ci}$ , for  $i = d, s, b$ . The NP loop functions are

<sup>1</sup>Reference [8] did not include in their fit updated CDF and D0 results for  $S_{\phi_{\psi}}$  [6], which showed improved consistency with the SM over previous results favoring nonzero  $\phi_s^\Delta$  [5].

<sup>2</sup>We neglect running between the scales  $m_t$ ,  $m_W$ , and  $m_{H^\pm}$ , integrating out these degrees of freedom at a common electroweak scale. Moreover, we have neglected a NP QCD correction factor  $\eta(x_H, x_t)/\eta_B$  arising at next-to-leading order [27].

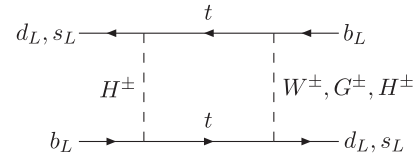


FIG. 1. New physics  $B_d^0$ - $\bar{B}_d^0$  and  $B_s^0$ - $\bar{B}_s^0$  mixing amplitudes  $(M_{12}^{d,s})_{\text{NP}}$  arising from box graphs with  $H^\pm$  exchange.

$$F_1(x_H, x_t) = \frac{x_t x_H (x_H - 4) \log x_H}{(x_H - 1)(x_H - x_t)^2} - \frac{x_t (x_t - 4)}{(x_t - 1)(x_H - x_t)} - \frac{x_t (x_H x_t^2 - 2x_H x_t + 4x_H - 3x_t^2) \log x_t}{(x_t - 1)^2 (x_H - x_t)^2}, \quad (12)$$

$$F_2(x_H, x_t) = \frac{x_H^2 - x_t^2 - 2x_t x_H \log(x_H/x_t)}{(x_H - x_t)^3}, \quad (13)$$

where  $x_{t,H} \equiv m_{t,H^\pm}^2/m_W^2$ , and  $S_0(x_t) \approx 2.35$  is the SM loop function (e.g., see [26]).

$B_{d,s}^0$ - $\bar{B}_{d,s}^0$  mixing from box graphs in a 2HDM have been computed previously [28]. Here, a novel feature arises from the NP  $CP$ -violating phase associated with  $\tilde{y}_{tc}$  [29]. We can write  $(\tilde{y}_U V)_{ii}$  as

$$\begin{aligned} (\tilde{y}_U V)_{tb} &\simeq \tilde{y}_{it} V_{tb}, \\ (\tilde{y}_U V)_{ts} &= \tilde{y}_{it} V_{ts} \left( 1 + \left| \frac{\tilde{y}_{tc} V_{cs}}{\tilde{y}_{it} V_{ts}} \right| e^{i\vartheta_{tc}} \right), \\ (\tilde{y}_U V)_{td} &= \tilde{y}_{it} V_{td} \left( 1 + \left| \frac{\tilde{y}_{tc} V_{cd}}{\tilde{y}_{it} V_{td}} \right| e^{i(\vartheta_{tc} + \beta)} \right), \end{aligned} \quad (14)$$

where  $\vartheta_{tc} \equiv \arg(\tilde{y}_{tc} V_{cs} \tilde{y}_{it}^* V_{ts}^*)$ . In the limit  $|\tilde{y}_{it}| \gg |\tilde{y}_{tc}|$ , we neglect the term  $\tilde{y}_{tc} V_{cb}$  for  $i = b$ ; however,  $y_{tc}$  is non-negligible for  $i = d, s$  because the  $\tilde{y}_{it}$  terms are Cabibbo suppressed.

The NP phase that enters  $(M_{12}^s)_{\text{NP}}$  is  $\vartheta_{tc}$ , while for  $(M_{12}^d)_{\text{NP}}$  it is  $(\vartheta_{tc} + \beta)$ , due to the different CKM structures of  $(\tilde{y}_U V)_{ts}$  and  $(\tilde{y}_U V)_{td}$ . The best fit values for  $\phi_{d,s}^\Delta$  are quite different numerically, but due to this extra  $e^{i\beta}$ , we can explain both  $\phi_{d,s}^\Delta$  in terms of the single NP phase  $\vartheta_{tc}$ . [For  $\tilde{y}_{tc} = 0$ , our model gives  $\phi_{d,s}^\Delta = 0$ , since  $(M_{12}^q)_{\text{NP}}$  would have the same complex phase  $(V_{tb} V_{tq}^*)^2$  as  $(M_{12}^q)_{\text{SM}}$ .]

Our results for  $B_{d,s}^0$ - $\bar{B}_{d,s}^0$  mixing are shown in Fig. 2. Here, we map best fit regions for  $\Delta_{d,s}$  from Ref. [8] into the parameter space of our model. We fix  $|\tilde{y}_{it}|$  and  $m_{H^\pm}$  and evaluate the preferred regions for  $|\tilde{y}_{tc}|$  and  $\vartheta_{tc}$  consistent with  $B_{d,s}^0$ - $\bar{B}_{d,s}^0$  mixing constraints. (As discussed below, EWBG favors  $|\tilde{y}_{it}| \sim 1$  and  $m_{H^\pm} \lesssim 500$  GeV.) The dark blue (light red) contours correspond to the best fit regions at  $1\sigma$  (inner) and  $2\sigma$  (outer), for  $\Delta_d$  ( $\Delta_s$ ). Since  $\Delta_{d,s}$  are quadratic functions of  $|\tilde{y}_{tc}| e^{i\vartheta_{tc}}$ , the best fit regions for  $\Delta_{d,s}$  each map into two best fit regions in  $|\tilde{y}_{tc}|, \vartheta_{tc}$  parameter space.

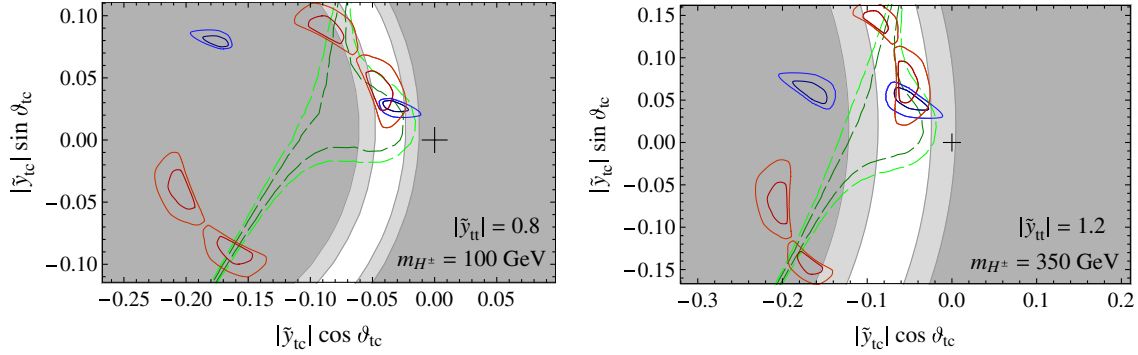


FIG. 2 (color online). Top-charm flavor violation parameter space  $(|\tilde{y}_t|, \vartheta_{tc})$  consistent with flavor observables, for two choices of  $|\tilde{y}_t|$ ,  $m_{H^\pm}$  68% and 95% C.L. regions for  $\Delta_d$  ( $\Delta_s$ ) from Ref. [8] shown by blue (red) contours. Region within dark (light) dashed green contours is consistent with  $\epsilon_K$  at 68% (95%) C.L. Light (dark) grey region is excluded at 68% (95%) C.L. from  $BR(\bar{B} \rightarrow X_s \gamma)$ .

We also implement constraints on our model from  $b \rightarrow s \gamma$  and  $\epsilon_K$ . The branching ratios for  $b \rightarrow s \gamma$ , as measured experimentally [30] and evaluated theoretically in the SM at next-to-leading order (NLO) [31], are given by<sup>3</sup>

$$\begin{aligned} BR[\bar{B} \rightarrow X_s \gamma]_{E_\gamma > 1.6 \text{ GeV}}^{\text{exp}} &= (3.55 \pm 0.24 \pm 0.09) \times 10^{-4}, \\ BR[\bar{B} \rightarrow X_s \gamma]_{E_\gamma > 1.6 \text{ GeV}}^{\text{SM}} &= (3.60 \pm 0.30) \times 10^{-4}. \end{aligned} \quad (15)$$

We evaluate SM + NP contributions to  $BR[\bar{B} \rightarrow X_s \gamma]$  in our model at NLO following Refs. [31,33], except that we take as inputs the best fit CKM parameters given in Table 11 of Ref. [8]. Adding all errors in Eqs. (15) in quadrature, we take the following constraint on our model:

$$BR[\bar{B} \rightarrow X_s \gamma]_{E_\gamma > 1.6 \text{ GeV}}^{\text{SM+NP}} = (3.55 \pm 0.39) \times 10^{-4}. \quad (16)$$

In Fig. 2, the white (light grey) region corresponds to  $|\tilde{y}_t|, \vartheta_{tc}$  parameter space consistent with Eq. (16) at less than  $1\sigma$  ( $2\sigma$ ), while the dark grey region is excluded at  $2\sigma$ .

NP contributions to  $K^0$ - $\bar{K}^0$  mixing arise in our model through box graphs analogous to Fig. 1. The strongest constraint is due to  $\epsilon_K$ . In the SM,  $|\epsilon_K|_{\text{SM}} = (1.90 \pm 0.26) \times 10^{-3}$  [34], while experimentally  $|\epsilon_K|_{\text{exp}} = (2.228 \pm 0.011) \times 10^{-3}$  [35]. The SM + NP value of  $\epsilon_K$  is

$$\begin{aligned} |\epsilon_K|_{\text{SM+NP}} &= \kappa_\epsilon C_\epsilon \hat{B}_K \text{Im}[(V_{ts} V_{td}^*)^2 \eta_2(S_0(x_t)) \\ &\quad + c_{sd} F_1(x_H, x_t) + c_{sd}^2 F_2(x_H, x_t)) \\ &\quad + (V_{cs} V_{cd}^*)^2 \eta_1 S_0(x_c) \\ &\quad + 2(V_{cs} V_{cd}^* V_{ts} V_{td}^*) \eta_3 S_0(x_c, x_t)], \end{aligned} \quad (17)$$

<sup>3</sup>In the observed value, the first error is experimental, while the second is a theoretical error associated with a photon shape function used to extrapolate the branching ratio to different photon energies  $E_\gamma$ . Also, although  $BR[\bar{B} \rightarrow X_s \gamma]$  has been computed at NNLO in the SM [32], we work at NLO since 2HDM contributions have been computed at NLO only.

where NP enters through the coefficients  $c_{sd}$  defined in Eq. (11). (We neglect NP NLO corrections to  $\eta_2$ .) The remaining SM input parameters in Eq. (17) are defined and tabulated in Ref. [8]. Assuming a theoretical error bar as in Ref. [34], we take the following constraint on our model:

$$|\epsilon_K|_{\text{SM+NP}} = (2.23 \pm 0.30) \times 10^{-3}. \quad (18)$$

It appears that since  $|\epsilon_K|_{\text{SM}} < |\epsilon_K|_{\text{exp}}$ , this constraint would favor a small, positive contribution from NP. However,  $|\epsilon_K|_{\text{SM}}$  itself is shifted to a central value  $|\epsilon_K|_{\text{SM}} = 2.40 \times 10^{-3}$  because the best fit CKM parameters in the presence of NP in  $B_{d,s}^0$ - $\bar{B}_{d,s}^0$  mixing (given in Table 11 of Ref. [8]) are different than in an SM-only fit. As a result, Eq. (18) favors a small, negative contribution from NP. In Fig. 2, the parameter region within the dashed dark (light) green contours is consistent with the  $\epsilon_K$  constraint in Eq. (18) at  $1\sigma$  ( $2\sigma$ ).

Here, we make several important points.

- (i) Despite the fact that  $\phi_d^\Delta$  and  $\phi_s^\Delta$  are quite different numerically, there exists regions of parameter space where *both* NP in  $B_d^0$ - $\bar{B}_d^0$  and  $B_s^0$ - $\bar{B}_s^0$  can be explained by a single phase  $\vartheta_{tc}$ . The  $1\sigma$  best fit regions for  $\Delta_{d,s}$  overlap within the parameter space of our model (neglecting correlations between  $\Delta_d$  and  $\Delta_s$ ).
- (ii) The  $\Delta_s$  region that overlaps with the  $\Delta_d$  region in Fig. 2 corresponds to the  $\phi_s^\Delta = (-51.6_{-9.4}^{+14.1})^\circ$  solution. Therefore, our model predicts  $\Delta\Gamma_s > 0$ .
- (iii) Although  $b \rightarrow s \gamma$  and  $\epsilon_K$  constrain a large parametric region of our model, these two observables are consistent with observation in regions favored by  $B$  mixing observables.
- (iv) A large phase  $\vartheta_{tc}$  can weaken  $b \rightarrow s \gamma$  and  $\epsilon_K$  constraints, and a light charged Higgs boson ( $m_{H^\pm} \sim 100$  GeV) is not excluded.
- (v) The values of  $(|\tilde{y}_t|, m_{H^\pm})$  shown in Fig. 2 are consistent with  $R_b \equiv BR[Z \rightarrow b\bar{b}]/BR[Z \rightarrow \text{hadrons}]$  at 95% C.L. [12].

Although we chose only two illustrative values  $(|\tilde{y}_t|, m_{H^\pm}) = (0.8, 100 \text{ GeV})$  and  $(1.2, 350 \text{ GeV})$  in



Fig. 2, there exists a consistency region between all these observables for parameters  $|\tilde{y}_H| \sim 1$ ,  $|\tilde{y}_{tc}| \sim 0.05\text{--}0.1$ , and  $\vartheta_{tc} \sim 3\pi/4$ , for  $100 < m_{H^\pm} < 500$  GeV. As we discuss below, EWBG favors  $|\tilde{y}_H| \sim 1$  and  $m_{H^\pm} \lesssim 500$  GeV.

#### IV. ELECTROWEAK BARYOGENESIS

Given an NP model, viable EWBG requires (1) the electroweak phase transition must be strongly first order to prevent washout of baryon number, and (2)  $CP$  violation must be sufficient to account for the observed baryon-to-entropy ratio  $Y_B^{\text{obs}} \approx 9 \times 10^{-11}$ . EWBG in a 2HDM has been studied many times previously [36]. Most recently, Ref. [37] showed that a strong first-order phase transition can occur in a type-II 2HDM for  $m_{H^0} \lesssim 200$  GeV and  $300 \lesssim m_{H^\pm} \lesssim 500$  GeV. Although our 2HDM is not exactly the same as in Ref. [37], we assume that a strong first-order transition does occur. (The phase transition can also be further strengthened or modified by the presence of scalar gauge singlets [38] or nonrenormalizable operators [39].)

We now study baryon number generation during the phase transition. The dynamical Higgs fields during the transition gives rise to a spacetime-dependent mass matrix  $M(x)$  for, e.g.,  $u$ -type quarks:

$$\begin{aligned} \mathcal{L}_{\text{mass}} &= -\bar{u}_R M u_L + \text{H.c.}, \\ M &= y_U v_1(T) + \tilde{y}_U v_2(T), \end{aligned} \quad (19)$$

where  $v_{1,2}(T) \equiv \langle H_{1,2}^0 \rangle_{T \neq 0}$  are the vevs at finite temperature  $T \approx 100$  GeV. At zero temperature, when  $v_1(T)$ ,  $v_2(T) \rightarrow v$ , 0, we recover the usual  $T = 0$  masses. However, if  $v_2(T) \neq 0$ , then  $CP$ -violating quark charge density can arise from  $\tilde{y}_U$ , as we show below. Left-handed quark charge, in turn, leads to baryon number production through weak sphalerons. In previous studies,  $CP$  asymmetries were generated by a spacetime-dependent Higgs vev phase, arising from  $CP$  violation in the Higgs sector [36,37]. Here, we assume that the Higgs potential is  $CP$ -conserving, such that  $v_{1,2}(T)$  do not have spacetime-dependent phases and can be taken to be real.

Is it plausible that  $v_2(T) \neq 0$  during the phase transition? Following [10], the most general potential for  $H_{1,2}$  can be written

$$\begin{aligned} V &= \lambda(H_1^\dagger H_1 - v^2)^2 + m_{H_2}^2 H_2^\dagger H_2 + \lambda_1 H_1^\dagger H_1 H_2^\dagger H_2 \\ &+ \lambda_2 H_1^\dagger H_2 H_2^\dagger H_1 + [\lambda_3(H_1^\dagger H_2)^2 + \lambda_4 H_1^\dagger H_2 H_2^\dagger H_2 \\ &+ \lambda_5 H_2^\dagger H_1 (H_1^\dagger H_1 - v^2) + \text{H.c.}] + \lambda_6 (H_2^\dagger H_2)^2 \end{aligned} \quad (20)$$

Our basis choice that  $\langle H_2^0 \rangle_{T=0} = 0$  requires that no terms linear in  $H_2$  survive when  $H_1^0 \rightarrow v$ . The same statement does not hold at  $T \neq 0$  due to thermal corrections to  $V$ . First, since we expect  $v_1(T) \neq v$ , terms linear in  $H_2$  appear proportional to  $\lambda_5$ . Second, top quark loops generate a

contribution to the potential  $(y_t \tilde{y}_H T^2 H_1^\dagger H_2/4 + \text{H.c.})$ , given here in the high  $T$  limit, also linear in  $H_2$ . A proper treatment of this issue requires a numerical evaluation of the bubble wall solutions of the finite  $T$  Higgs potential, which is beyond the scope of this project. Here, we treat  $\tan\beta(T) \equiv v_2(T)/v_1(T)$  as a free parameter,<sup>4</sup> and we work in the  $\beta(T) \ll 1$  limit. Intuitively, we expect  $\beta(T)$  to be suppressed in the limit  $m_{H_2}^2 \gg T^2$ , since the vev will be confined along the  $\langle H_2^0 \rangle = 0$  valley.

The charge transport dynamics of EWBG are governed by a system of Boltzmann equations of the form  $\dot{n}_a = S_a^{\mathcal{CP}} + D_a \nabla^2 n_a + \sum_b \Gamma_{ab} n_b$  [40]. Here  $n_a$  is the charge density for species  $a$ . The  $CP$ -violating source  $S_a^{\mathcal{CP}}$  generates nonzero  $n_a$  within the expanding bubble wall, at the boundary between broken and unbroken phases, due to the spacetime-varying vevs  $v_{1,2}(T)$ . The diffusion constant  $D_a$  describes how  $n_a$  is transported ahead of the wall into the unbroken phase, where weak sphalerons are active. The remaining terms describe inelastic interactions that convert  $n_a$  into charge density of other species  $b$ , with rate  $\Gamma_{ab}$ . Our setup of the Boltzmann equations follows standard methods, described in detail in Ref. [41].

Following Ref. [40], we assume a planar bubble wall geometry, with velocity  $v_w \ll 1$  and coordinate  $z$  normal to the wall. The  $z > 0$  ( $z < 0$ ) region corresponds to the (un)broken phase. We look for steady state solutions in the rest frame of the wall that only depend on  $z$ . Therefore, we replace  $\dot{n}_a \rightarrow v_w n'_a$  and  $\nabla^2 n_a \rightarrow n''_a$ , where prime denotes  $\partial/\partial z$ . We adopt kink bubble wall profiles

$$v(T)/T = \xi[1 + \tanh(z/L_w)]/(2\sqrt{2}), \quad (21)$$

$$\beta(T) = \Delta\beta[1 + \tanh(z/L_w)]/2, \quad (22)$$

where  $v(T)^2 \equiv v_1(T)^2 + v_2(T)^2$ . We take  $\xi = 1.5$ , wall width  $L_w = 5/T$ , and  $T = 100$  GeV. Reference [37] found viable first-order phase transitions with  $1 < \xi < 2.5$  and  $2 < L_w T < 15$ , depending on the Higgs parameters. For definiteness, we take  $m_{H_2} = 400$  GeV; however, our analysis does not account for the crucially important  $m_{H_2}$  dependence of the bubble profiles.

Specializing to our 2HDM, the complete set of Boltzmann equations is

$$\begin{aligned} v_w n'_{q_a} &= D_q n''_{q_a} + \delta_{3a}(S_t^{\mathcal{CP}} + \Gamma_y \mathcal{Q}_y + \Gamma_m \mathcal{Q}_m) - 2\Gamma_{ss} \mathcal{Q}_{ss}, \\ v_w n'_{u_a} &= D_q n''_{u_a} - \delta_{3a}(S_t^{\mathcal{CP}} + \Gamma_y \mathcal{Q}_y + \Gamma_m \mathcal{Q}_m) + \Gamma_{ss} \mathcal{Q}_{ss}, \\ v_w n'_{d_a} &= D_q n''_{d_a} + \Gamma_{ss} \mathcal{Q}_{ss}, \\ v_w n'_H &= D_H n''_H + \Gamma_y \mathcal{Q}_y - \Gamma_h \mathcal{Q}_h, \end{aligned} \quad (23)$$

with linear combinations of charge densities

<sup>4</sup>Although the usual  $\tan\beta$  is not physical at  $T = 0$ , the angle  $\beta(T)$  between the  $T = 0$  and  $T \neq 0$  vev directions is physical.

$$Q_y \equiv \frac{n_{u_3}}{k_{u_3}} - \frac{n_{q_3}}{k_{q_3}} - \frac{n_H}{k_H}, \quad Q_m \equiv \frac{n_{u_3}}{k_{u_3}} - \frac{n_{q_3}}{k_{q_3}}, \quad (24)$$

$$Q_{ss} \equiv \sum_{a=1}^3 \left( \frac{2n_{q_a}}{k_{q_a}} - \frac{n_{u_a}}{k_{u_a}} - \frac{n_{d_a}}{k_{d_a}} \right), \quad Q_h = \frac{n_H}{k_H}.$$

The relevant densities are the  $a$ th generation left(right)-handed quark charges  $n_{q_a}$  ( $n_{u_a}$ ,  $n_{d_a}$ ), and the Higgs charge density  $n_H \equiv n_{H_1} + n_{H_2}$  (we treat  $H_{1,2}$  as mass eigenstates in the unbroken phase). We assume that (Cabibbo unsuppressed) gauge interactions are in equilibrium, as are Higgs interactions that chemically equilibrate  $H_{1,2}$  (provided by  $\lambda_{3,4,5}$  quartic couplings in  $V$ ). Lepton densities do not get sourced and can be neglected. The  $k$  factors are defined by  $n_a = T^2 k_a \mu_a / 6$ , with chemical potential  $\mu_a$ .

In the Eqs. (23), we take these transport coefficients as input:

$$S_t^{\mathcal{CP}} \approx 0.1 \times N_c |y_t \tilde{y}_t| \sin \theta_{tt} v(T)^2 v_w \beta(T) T, \quad (26)$$

$$\Gamma_m \approx 0.1 \times N_c |y_t v_1(T) + \tilde{y}_t v_2(T)|^2 T^{-1}, \quad (27)$$

$$\Gamma_y \approx \frac{27 \zeta_3^2}{2\pi^2} \alpha_s y_t^2 T + 9 |\tilde{y}_t|^2 T \left( \frac{m_{H_2}}{2\pi T} \right)^{5/2} e^{-m_{H_2}/T}, \quad (28)$$

$$\Gamma_{ss} \approx 14 \alpha_s^4 T, \quad D_q \approx 6/T, \quad D_H \approx 100/T. \quad (29)$$

We compute the  $CP$ -violating source  $S_t^{\mathcal{CP}}$  and relaxation rate  $\Gamma_m$ , arising for  $t_{L,R}$  only, following the vev-insertion formalism [42,43] (explicit formulas can be found in [44]).<sup>5</sup> The sole source of  $CP$  violation here is the phase  $\theta_{tt} \equiv \arg(\tilde{y}_t)$ , which is *not* the same phase that enters into  $B_{d,s}^0 - \bar{B}_{d,s}^0$  mixing.<sup>6</sup> The dimensionless numerical factors (0.1), obtained following Ref. [43], arise from integrals over  $t_{L,R}$  quasiparticle momenta, taking as input the thermal masses (tabulated in [46]) and thermal widths ( $\gamma_{t_{L,R}} \approx 0.15 g_s^2 T$  [47]). The top Yukawa rate  $\Gamma_y$  comes from processes  $H_1 t_L \leftrightarrow t_R g$  and  $H_2 \leftrightarrow t_R \tilde{t}_L$  [46,48]. The strong sphaleron rate  $\Gamma_{ss}$  [49] plays a crucial role in EWBG in the 2HDM [50], discussed below, and  $D_{q,H}$  are the quark and Higgs diffusion constants [51]. The relaxation rate  $\Gamma_h$  is due to Higgs charge nonconservation when the vev is nonzero. For simplicity, we set  $\Gamma_h = \Gamma_m$  [40]; we find deviations from this estimate lead to  $\lesssim \mathcal{O}(1)$  variations in our computed  $Y_B$ . We have omitted from Eq. (23) additional Yukawa interactions induced by  $y_{tc}$  (e.g.,  $H_2 \leftrightarrow t_R \tilde{c}_L$ ) because we find they have negligible impact on  $Y_B$ . Moreover,  $CP$ -violating sources from  $y_{tc}$  do not arise at leading order in vev insertions. Therefore,  $y_{tc}$  plays

<sup>5</sup>Although there exist more sophisticated treatments, the reliability of quantitative EWBG computations remains an open question (see discussion in [45]).

<sup>6</sup>The reparametrization invariant phase is  $\theta_{tt} \equiv \arg(\tilde{y}_t y_t^* v_1^* v_2)$ , but we have adopted a convention where  $v_{1,2}(T)$  and  $y_t$  are real and positive.

no role in our EWBG setup (this conclusion may not hold beyond the vev-insertion formalism).

Thus far, we have neglected baryon number violation; this is reasonable since the weak sphaleron rate  $\Gamma_{ws} \approx 120 \alpha_w^5 T$  [52] is slow and out of equilibrium. Therefore, we solve for the total left-handed charge  $n_L \equiv \sum_a n_{q_a}$  from Eqs. (23), neglecting  $\Gamma_{ws}$ , and then treat  $n_L$  as a source for baryon density  $n_B$ , according to

$$v_w n_B' - D_q n_B'' = -(3\Gamma_{ws} n_L + \mathcal{R} n_B) h, \quad (30)$$

with the relaxation rate  $\mathcal{R} = (15/4)\Gamma_{ws}$  [53]. The sphaleron profile  $h(z)$  governs how  $\Gamma_{ws}$  turns off in the broken phase [54]. Since the energy of the  $T = 0$  sphaleron is  $E_{\text{sph}} \approx 4M_W/\alpha_w$ , we take [55]

$$h(z) = \exp(-E_{\text{sph}}(T)/T), \quad E_{\text{sph}}(T) = E_{\text{sph}} v(T)/v. \quad (31)$$

Effectively, this cuts off the weak sphaleron rate for relatively small values of the vev:  $v(T, z)/T \gtrsim g_2/(8\pi)$ .

In Fig. 3, we show the spatial charge densities resulting from a numerical solution to Eqs. (23) for an example choice of parameters giving  $Y_B \approx 9 \times 10^{-11}$ . In general, the individual charge densities have long diffusion tails into the unbroken phase ( $z < 0$ ). However,  $n_L$  is strongly localized near the bubble wall ( $z = 0$ ), due to strong sphalerons, thereby suppressing  $n_B$  [50]. This effect can be understood as follows: at the level of Eqs. (23),  $B$  is conserved, implying  $\sum_a (n_{q_a} + n_{u_a} + n_{d_a}) = 0$ ; additionally, strong sphalerons relax the linear combination of densities

$$Q_{ss} \approx (1/N_c) \sum_a (n_{q_a} - n_{u_a} - n_{d_a}) \quad (32)$$

to zero. These considerations imply that  $n_L \approx 0$  if strong sphalerons are in equilibrium. In Fig. 3, we see that strong sphalerons are equilibrated and  $n_L$  vanishes for  $z \lesssim -10L_w$ . Since  $n_L$  is nonzero only near the wall, it is important to treat the weak sphaleron profile accurately in this region, rather than with a simple step function. Nevertheless, despite this suppression, EWBG can account

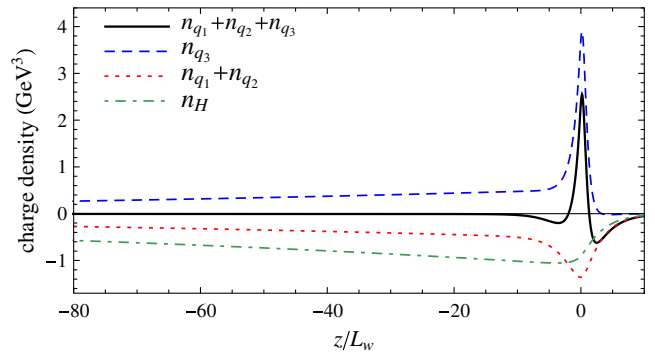


FIG. 3 (color online). Charge densities in the unbroken phase ( $z < 0$ ) for  $|\tilde{y}_t| = 1$ ,  $\theta_{tt} = 0.18$ ,  $v_w = 0.05$ ,  $\Delta\beta = 10^{-2}$ , giving  $Y_B \approx 9 \times 10^{-11}$ .

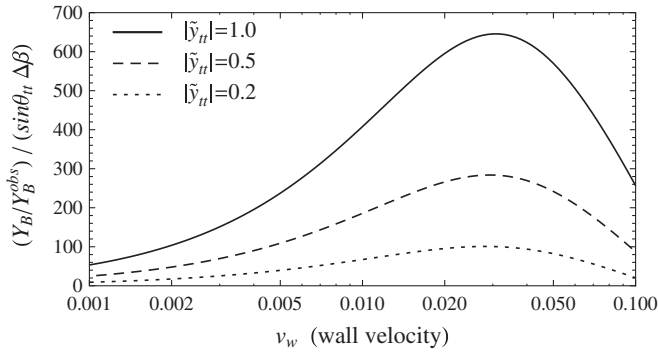


FIG. 4. Computed baryon asymmetry  $Y_B$ , normalized with respect to  $Y_B^{\text{obs}} \sim 9 \times 10^{-11}$  and  $(\sin\theta_H \Delta\beta)$ , as a function of  $v_w$  and  $|\tilde{y}_H|$ . Vertical axis shows  $(\sin\theta_H \Delta\beta)^{-1}$ , required for viable EWBG.

for  $Y_B^{\text{obs}}$ . (We also note the significant Higgs charge  $n_H$  in the broken phase. Although we neglect lepton Yukawas here, it is possible that  $n_H$  could be efficiently transferred into left-handed lepton charge via  $\tilde{y}_L$ , thereby driving EWBG without suffering from strong sphaleron suppression, analogous to Ref. [46].)

In Fig. 4, we show how large  $Y_B$  can be in our model. The most important parameters are  $\Delta\beta$ ,  $\tilde{y}_H$ , and  $v_w$  (we find  $Y_B$  is not strongly sensitive to  $L_w$  or  $\xi$ ). The vertical axis shows the (inverse) value of  $\Delta\beta \times \sin\theta_H$  required for successful EWBG ( $Y_B = Y_B^{\text{obs}}$ ), for different values of  $|\tilde{y}_H|$  and  $v_w$ . Our main conclusion is that our model can easily account for the baryon asymmetry of the Universe—even if  $\Delta\beta$  is as small as  $10^{-3} - 10^{-2}$ , provided the NP Yukawa coupling has magnitude  $|\tilde{y}_H| \gtrsim 0.2$ , with  $\mathcal{O}(1)$  phase. Moreover,  $|\tilde{y}_H| \sim 1$  is preferred by consistency with flavor observables.

## V. CONCLUSIONS

The dimuon asymmetry reported by D0 [2] and the branching ratio  $\text{BR}(B \rightarrow \tau\nu)$  [3,4] seem to disfavor the CKM paradigm of  $CP$  violation in the SM at the  $\sim 3\sigma$  level. Although more experimental scrutiny is required, taken at face value, these anomalies can be accounted for by new physics in both  $B_d^0$ - $\bar{B}_d^0$  and  $B_s^0$ - $\bar{B}_s^0$  mixing [8]. Such new physics would involve new weak-scale bosonic degrees of freedom and new large  $CP$ -violating phases. These two ingredients are precisely what is required for viable electroweak baryogenesis in extensions of the SM.

We proposed a simple 2HDM that can account for these  $B$  meson anomalies and the baryon asymmetry. An interesting feature of our setup is a top-charm flavor-violating Yukawa coupling of the new physics Higgs doublet. The large relative phase of this coupling can explain *both* the dimuon asymmetry and tension in  $\text{BR}(B \rightarrow \tau\nu)$ . Although top-charm flavor violation can give potentially large contributions to  $b \rightarrow s\gamma$  and  $\epsilon_K$  (i.e., less CKM-suppressed than SM contributions), these bounds are weakened in precisely the same region of parameter space consistent with  $B_{d,s}^0$ - $\bar{B}_{d,s}^0$  observables.

We also discussed electroweak baryogenesis. We showed that, provided a strong first-order electroweak phase transition occurs, our model can easily explain the observed baryon asymmetry of the Universe.  $CP$  violation during the phase transition is provided by the relative phase in the flavor-diagonal  $t_L$ - $t_R$  Yukawa coupling  $\tilde{y}_H$  to the new Higgs boson, and the relevant phase is not related to the top-charm  $CP$  phase entering flavor observables. However, flavor observables and baryogenesis both require  $|\tilde{y}_H| \sim 1$ . Additionally, baryon generation is dependent on a parameter  $\Delta\beta$  related to the shift in the ratio of Higgs vevs across the bubble wall. We expect  $\Delta\beta$  to be suppressed in the limit  $m_{H^\pm} \gg m_w$ . However, we showed that the charged Higgs state  $H^\pm$  can be light ( $m_{H^\pm} \sim 100$  GeV) without conflicting with flavor observables due to the large top-charm phase in our model (as opposed to the limit  $m_{H^\pm} > 315$  GeV from  $b \rightarrow s\gamma$  in a type-II 2HDM [31,35]).

It would be interesting to explore the consequences of our model for Higgs- and top-related  $CP$ -violating and flavor-violating observables measurable in colliders, and also for rare decays such as  $K \rightarrow \pi\nu\bar{\nu}$ . Additionally, a more robust analysis of EWBG requires an analysis of the finite temperature effective potential in a type-III 2HDM, addressing the phase transition strength and bubble wall profiles.

## ACKNOWLEDGMENTS

We thank the authors of Ref. [8] for sharing with us numerical data from their global fit analysis. We are also indebted to K. Blum, V. Cirigliano, J. Cline, Y. Hochberg, D. Morrissey, Y. Nir, M. Pospelov, and M. Trott for helpful discussions and suggestions. S. T. is supported by NSERC of Canada.

- [1] M. Kobayashi and T. Maskawa, *Prog. Theor. Phys.* **49**, 652 (1973).
- [2] V. M. Abazov *et al.* (D0 Collaboration), *Phys. Rev. D* **82**, 032001 (2010).
- [3] O. Deschamps, [arXiv:0810.3139](https://arxiv.org/abs/0810.3139).

- [4] E. Lunghi and A. Soni, *Phys. Lett. B* **697**, 323 (2011).
- [5] V. M. Abazov *et al.* (D0 Collaboration), *Phys. Rev. Lett.* **101**, 241801 (2008); D0 Collaboration, Conference Notes Report No. 5928-CONF; CDF Collaboration, Public Notes



- Report Nos. 9458, 9787; G. Punzi, Proc. Soc., EPS-HEP2009 (2009) 022.
- [6] D0 Collaboration, Conference Note Report No. 6098-CONF; CDF Collaboration, Public Note Report No. 10206.
- [7] Z. Ligeti, M. Papucci, G. Perez, and J. Zupan, *Phys. Rev. Lett.* **105**, 131601 (2010); C. W. Bauer and N. D. Dunn, *Phys. Lett. B* **696**, 362 (2011); A. K. Alok, S. Baek, and D. London, arXiv:1010.1333; N. G. Deshpande, X. -G. He, and G. Valencia, *Phys. Rev. D* **82**, 056013 (2010); K. Blum, Y. Hochberg, and Y. Nir, *J. High Energy Phys.* **09** (2010) 035; B. Batell and M. Pospelov, *Phys. Rev. D* **82**, 054033 (2010).
- [8] A. Lenz *et al.*, *Phys. Rev. D* **83**, 036004 (2011).
- [9] B. A. Dobrescu, P. J. Fox, and A. Martin, *Phys. Rev. Lett.* **105**, 041801 (2010).
- [10] M. Trott and M. B. Wise, *J. High Energy Phys.* **11** (2010) 157.
- [11] A. J. Buras, G. Isidori, and P. Paradisi, *Phys. Lett. B* **694**, 402 (2011).
- [12] M. Jung, A. Pich, and P. Tuzon, *J. High Energy Phys.* **11** (2010) 003.
- [13] M. E. Shaposhnikov, *Nucl. Phys.* **B287**, 757 (1987).
- [14] A. G. Cohen, D. B. Kaplan, and A. E. Nelson, *Annu. Rev. Nucl. Part. Sci.* **43**, 27 (1993).
- [15] V. A. Kuzmin, V. A. Rubakov, and M. E. Shaposhnikov, *Phys. Lett.* **155B**, 36 (1985).
- [16] A. D. Sakharov, *Pisma Zh. Eksp. Teor. Fiz.* **5**, 32 (1967).
- [17] Y. Aoki, F. Csikor, Z. Fodor, and A. Ukawa, *Phys. Rev. D* **60**, 013001 (1999); K. Kajantie, M. Laine, K. Rummukainen, and M. E. Shaposhnikov, *Nucl. Phys.* **B466**, 189 (1996).
- [18] M. B. Gavela, M. Lozano, J. Orloff, and O. Pene, *Nucl. Phys.* **B430**, 345 (1994); M. B. Gavela, P. Hernandez, J. Orloff, O. Pene, and C. Quimbay, *Nucl. Phys.* **B430**, 382 (1994); P. Huet and E. Sather, *Phys. Rev. D* **51**, 379 (1995).
- [19] M. Pospelov and A. Ritz, *Ann. Phys. (N.Y.)* **318**, 119 (2005).
- [20] F. R. Klinkhamer and N. S. Manton, *Phys. Rev. D* **30**, 2212 (1984).
- [21] G. Isidori, Y. Nir, and G. Perez, arXiv:1002.0900.
- [22] T. D. Lee, *Phys. Rev. D* **8**, 1226 (1973); W.-S. Hou, *Phys. Lett. B* **296**, 179 (1992); D. Atwood, L. Reina, and A. Soni, *Phys. Rev. D* **55**, 3156 (1997); S. Davidson and H. E. Haber, *Phys. Rev. D* **72**, 035004 (2005).
- [23] T. P. Cheng and M. Sher, *Phys. Rev. D* **35**, 3484 (1987).
- [24] H. E. Haber and D. O'Neil, *Phys. Rev. D* **74**, 015018 (2006).
- [25] I. I. Bigi and A. I. Sanda, *CP Violation* (Cambridge University Press, Cambridge, England, 2009), p. 485.
- [26] A. J. Buras, arXiv:hep-ph/9806471.
- [27] J. Urban, F. Krauss, U. Jentschura, and G. Soff, *Nucl. Phys.* **B523**, 40 (1998).
- [28] W.-S. Hou and R. S. Willey, *Nucl. Phys.* **B326**, 54 (1989).
- [29] R. A. Diaz, R. Martinez, and C. E. Sandoval, *Eur. Phys. J. C* **46**, 403 (2006).
- [30] D. Asner *et al.* (Heavy Flavor Averaging Group Collaboration), arXiv:1010.1589.
- [31] P. Gambino and M. Misiak, *Nucl. Phys.* **B611**, 338 (2001).
- [32] M. Misiak and M. Steinhauser, *Nucl. Phys.* **B764**, 62 (2007).
- [33] M. Ciuchini, G. Degrassi, P. Gambino, and G. F. Giudice, *Nucl. Phys.* **B527**, 21 (1998).
- [34] J. Brod and M. Gorbahn, *Phys. Rev. D* **82**, 094026 (2010).
- [35] K. Nakamura *et al.* (Particle Data Group Collaboration), *J. Phys. G* **G37**, 075021 (2010).
- [36] A. I. Bochkarev, S. V. Kuzmin, and M. E. Shaposhnikov, *Phys. Lett. B* **244**, 275 (1990); M. Dine, P. Huet, R. L. Singleton, Jr, and L. Susskind, *Phys. Lett. B* **257**, 351 (1991); A. G. Cohen, D. B. Kaplan, and A. E. Nelson, *Phys. Lett. B* **263**, 86; N. Turok and J. Zadrozny, *Nucl. Phys.* **B358**, 471 (1991); K. Funakubo, A. Kakuto, and K. Takenaga, *Prog. Theor. Phys.* **91**, 341 (1994). A. T. Davies, C. D. Froggatt, G. Jenkins, and R. G. Moorhouse, *Phys. Lett. B* **336**, 464 (1994); J. M. Cline, K. Kainulainen, and A. P. Vischer, *Phys. Rev. D* **54**, 2451 (1996).
- [37] L. Fromme, S. J. Huber, and M. Seniuch, *J. High Energy Phys.* **11** (2006) 038.
- [38] S. Profumo, M. J. Ramsey-Musolf, and G. Shaughnessy, *J. High Energy Phys.* **08** (2007) 010; D. J. H. Chung and A. J. Long, *Phys. Rev. D* **81**, 123531 (2010).
- [39] C. Grojean, G. Servant, and J. D. Wells, *Phys. Rev. D* **71**, 036001 (2005).
- [40] A. G. Cohen, D. B. Kaplan, and A. E. Nelson, *Phys. Lett. B* **336**, 41 (1994).
- [41] D. J. H. Chung, B. Garbrecht, M. J. Ramsey-Musolf, and S. Tulin, *J. High Energy Phys.* **12** (2009) 067.
- [42] A. Riotto, *Phys. Rev. D* **58**, 095009 (1998).
- [43] C. Lee, V. Cirigliano, and M. J. Ramsey-Musolf, *Phys. Rev. D* **71**, 075010 (2005).
- [44] K. Blum, C. Delaunay, M. Losada, Y. Nir, and S. Tulin, *J. High Energy Phys.* **05** (2010) 101.
- [45] V. Cirigliano, C. Lee, M. J. Ramsey-Musolf, and S. Tulin, *Phys. Rev. D* **81**, 103503 (2010); V. Cirigliano, C. Lee, M. J. Ramsey-Musolf, and S. Tulin (unpublished).
- [46] D. J. H. Chung, B. Garbrecht, M. J. Ramsey-Musolf, and S. Tulin, *Phys. Rev. D* **81**, 063506 (2010).
- [47] E. Braaten and R. D. Pisarski, *Phys. Rev. D* **46**, 1829 (1992).
- [48] P. Huet and A. E. Nelson, *Phys. Rev. D* **53**, 4578 (1996); V. Cirigliano, M. J. Ramsey-Musolf, S. Tulin, and C. Lee, *Phys. Rev. D* **73**, 115009 (2006).
- [49] G. D. Moore and M. Tassler, *J. High Energy Phys.* **02** (2011) 105.
- [50] G. F. Giudice and M. E. Shaposhnikov, *Phys. Lett. B* **326**, 118 (1994).
- [51] M. Joyce, T. Prokopec, and N. Turok, *Phys. Rev. D* **53**, 2930 (1996).
- [52] D. Bodeker, G. D. Moore, and K. Rummukainen, *Phys. Rev. D* **61**, 056003 (2000).
- [53] J. M. Cline, M. Joyce, and K. Kainulainen, *J. High Energy Phys.* **07** (2000) 018.
- [54] M. Dine and S. D. Thomas, *Phys. Lett. B* **328**, 73 (1994).
- [55] S. Braibant, Y. Brihaye, and J. Kunz, *Int. J. Mod. Phys. A* **8**, 5563 (1993).